Magnetic Resonance Characterization of Betaine Micelles and Betaine−Perfluoropolyether Mixed Vesicles

Sandra Ristori,[†] Cristiana Maggiulli,[†] Jacqueline Appell,[‡] Giuseppe Marchionni,[§] and Giacomo Martini*,[†]

Dipartimento di Chimica, Universitá di Firenze, 50121 Firenze, Italy, G.D.P.C. (UMR CNRS) case 26, Université de Montpellier II, F-34095 Montpellier Cedex 05, France, and Ausimont S.p.A., Research & Development, 20021 Bollate, Milano, Italy

Received: November 8, 1996; In Final Form: March 10, 1997[⊗]

Direct (dynamic and static light scattering, LS, and nuclear magnetic resonance, NMR) and indirect (electron spin resonance, ESR) techniques allowed us to obtain details on the dynamics and on the structure of betaine micelles and on mixed betaine−perfluoropolyether (PFPE) vesicles. The mixed vesicles formed in a very restricted range of total surfactant concentration and of betaine mole fraction. The occurrence of unilamellar, monodisperse vesicles has been previously shown by LS measurements (Ristori, S.; Appell, J.; Porte, G. *Langmuir* **1996**, *12*, 686). ESR from hydrogenated probes (*n*-doxylstearic acids, *n*-DXSA) suggested that separate domains existed in the vesicles, and these radicals localized in the betaine-rich domain. A perfluorinated nitroxide radical was synthesized to study the PFPE domain. From the ESR line shapes the dynamic features of the supramolecular assemblies were obtained. Static LS and QELS (quasi-elastic light scattering) ruled out that the addition of nitroxides in the systems under study had a significant effect on their size and shape. The structural features of the vesicles were also studied by 200-MHz ^{1}H-NMR experiments. On the basis of the structural and dynamic data obtained, a model is presented for the structure of unilamellar betaine/PFPE mixed vesicles. These systems can be used as stable carriers for drugs and biological molecules.

1. Introduction

Stable vesicles can be formed spontaneously, i.e. without either mechanical treatment, such as high-energy sonication, french pressure cell, high-pressure extrusion, or chemical treatment, such as detergent depletion, reverse phase separation, etc. These vesicles allow us to strongly simplify the steps necessary to produce objects suitable as carriers of pharmacologically or biologically active substances. The spontaneous formation of vesicles from surfactant bilayers has been obtained in some cases by using gangliosides as surfactants[1,2] and mixtures of anionic and cationic surfactants, of nonionic surfactants, and of nonionic surfactants doped with anionic surfactants.[3−8]

Perfluorinated compounds are largely used for preparing vesicles that are also used as carriers in biological fluids.[9−14] Very recently mixed vesicles were fabricated in a spontaneous way with a hydrogenated surfactant, namely, *n*-dodecylbetaine, and a perfluorinated surfactant, namely, a perfluoropolyether (PFPE).[15] These systems have been characterized mainly by static light scattering (LS) and quasi-elastic light scattering (QELS). Water dispersions of PFPE and other perfluorinated surfactants are known to give micellar and liquid crystal phases (lamellar phases). These have been investigated by magnetic resonance spectroscopies and small-angle X-ray and neutron scattering.[16−21]

The phase diagram for the PFPE/betaine system in 0.1 M NH_4Cl brine was determined in the dilute region in which monodisperse vesicles occur with polydisperse aggregates of unknown nature and mixed micellar aggregates.[15] The predominance of monodisperse, unilamellar vesicles with respect to the other aggregates depends on the total concentration of surfactants and on the betaine/PFPE molar ratio. Whereas in pure betaine solution above the critical micellar solution (cmc $= 2 \times 10^{-3}$ mol/L) small globular micelles (with a hydrodynamic radius $r_h \approx 2$ nm) are known to exist,[22] the addition of small amounts of PFPE leads to a steady increase of the micelle size (up to $r_h = 7-9$ nm), which are probably elongated micelles. In a very narrow range of betaine/PFPE molar ratios (from 0.7 to 0.8), spontaneous, unilamellar vesicles of well-defined sizes occur with r_h ranging from 70 to 130 nm at a total surfactant concentration increasing from 0.25% w/w to 1.27% w/w. The formation and the stability of these vesicles are discussed in terms of the model of Fattal *et al.*[23] for the transition from globular or cylindrical micelles to an infinite bilayer. This model neglects the curvature energy and elasticity, which are theoretically considered by Safran et al.,[24] Koslov and Helfrich,[25] and Porte and Ligoure[26] for systems containing only one surfactant. According to Safran and co-workers,[24] a partial miscibility of the two components of a vesicle may introduce an asymmetry in the system. The different composition of the inner and outer monolayers results in different spontaneous curvatures with a favorable bending of the bilayer.

In this paper we used magnetic resonance spectroscopies to investigate if two different domains exist in the betaine/PFPE mixed systems, the first one being composed mainly of betaine and the second mainly composed of PFPE. Electron spin resonance (ESR) of hydrogenated spin probes, namely, doxylstearic acids, gave information on the hydrogenated (betaine-rich) domain. A perfluorinated spin probe was synthesized for the study of the perfluorinated (PFPE-rich) domain. ^{1}H-NMR (200-MHz) of betaine, from pure betaine solutions in premicellar and micellar phases to mixed vesicles, allowed us to complete the picture of the vesicle status.

* Corresponding author.
[†] Universitá di Firenze.
[‡] Université de Montpellier II.
[§] Ausimont S.p.A.
[⊗] Abstract published in *Advance ACS Abstracts,* April 15, 1997.

S1089-5647(96)03745-5 CCC: $14.00

2. Experimental Section

Materials. Perfluoropolyether, with the following molecular scheme,

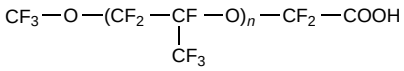

with $n = 3$, MW = 681, density = 1.8 kg/L, was prepared and characterized as a pure compound in the laboratories of Ausimont S.p.A., Bollate (Milano), Italy. It was used as the ammonium salt.[27] The salt was prepared from the PFPE in the acidic form by treating with excess ammonia. The excess ammonia was removed by simple heating. The precipitate was then washed several times with twice-distilled water and heated at 70 °C under vacuum for several hours.

n-Dodecylbetaine,

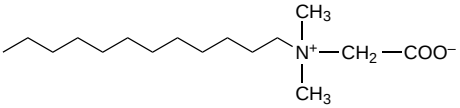

was synthesized and purified as a zwitterionic surfactant (MW = 271, density = 0.93 kg/L)[28] and used as prepared.

Mixtures of the above two surfactants were prepared in twice-distilled (Milli-Q) water containing 0.1 M NH_4Cl. Even if the occurrence of bilayer-type aggregates, such as vesicles and lamellar phases, was first obtained for pure water solutions,[29] we chose to work in brine because the presence of salt strongly decreases interactions among aggregates.

Mixed vesicles for the present study were prepared at total surfactant concentrations in the range 0.25−1.27% w/w, which was a well-characterized region of the ternary phase diagram.[15] The procedure given in ref 15 was usually followed.

The spin probes used were doxylstearic acid derivatives:

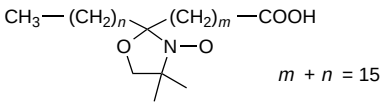

where

$n = 12$	$m = 3$	5-DXSA
$n = 10$	$m = 5$	7-DXSA
$n = 7$	$m = 8$	10-DXA
$n = 5$	$m = 10$	12-DXSA
$n = 1$	$m = 14$	16-DXSA

These spin probes, as well as Tempamine (4-amino-2,2,6,6-tetramethylpiperidine-1-oxyl), were obtained from Sigma Chemicals, München, Germany, and were used without further treatment. Their solutions were prepared in ethanol, acetone, or chloroform, depending on their use.

Tempamine was used for the preparation of the radical PFPE−Tempamide:

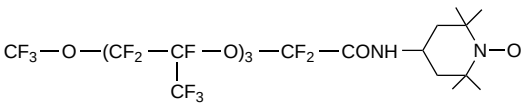

This compound was prepared from the acyl-chloride of PFPE and Tempamine according to the following schemes:

$$\mathrm{RCOOH} + \mathrm{SOCl_2} \rightarrow \mathrm{RCOCl} + \mathrm{HCl} + \mathrm{SO_2}$$

$$\mathrm{RCOCl} + \mathrm{R'NH_2} \rightarrow \mathrm{RCONHR'} + \mathrm{HCl}$$

In the reaction vessel, the PFPE acid (0.9458 g) was treated drop-by-drop with thionyl chloride (0.223 g) under stirring for 30 min and then heated at 80 °C under nitrogen moderate flux in order to remove excess $SOCl_2$. To the mixture, pyridine (0.6 g) was added at room temperature prior to the eventual addition of Tempamine (0.2527 g). In these conditions, the formation of Tempamonium chloride was prevented, since PyH^+Cl^- was favored and the amine was therefore available for a quantitative reaction with RCOCl. After 30 min of stirring, the reacted mass was washed with 10 cm^3 of H_2O and 5 cm^3 of CH_2Cl_2; excess pyridine, the unreacted acid chloride, the pyridinium hydrochloride, and the PFPE−pyridinium salt were thus solubilized. After a further washing with water and CH_2Cl_2 and vigorous stirring, the mass was centrifuged; 0.3 g of product was obtained and analyzed by ^{19}F-NMR, ^{1}H-NMR, and IR, which proved the presence of the desired PFPE−amide.[30] No further purification was made because it was not necessary for the use of the labeled PFPE.

Instrumentation. ESR spectra were registered with a Bruker spectrometer Model 200D (∼9.5 GHz, X-band). Temperature was controlled by a Bruker ST 100/700 variable temperature assembly. The accuracy was ±0.5 °C.

The introduction of the spin probes into the samples to be analyzed by ESR was achieved by simple evaporation of the desired amount of the solution of the probe on the bottom of a vial and subsequent addition of the vesicle solution to be studied. As an alternative route, vesicles were prepared by adding the PFPE solution directly in the vial containing the spin probe dissolved in the betaine solution. No difference in the results was observed. This latter procedure was preferred when molecules such as polyazamacrocycles and proteins were to be introduced into the vesicles.[31] The mixture was eventually stirred for at least 12 h at room temperature. Quartz samples of an inner diameter of 1−2 mm were used for ESR measurements.

^{1}H-NMR (200-MHz) spectra were recorded with a Bruker MSL-200 spectrometer using TMS (tetramethylsilane) as an external standard. D_2O solutions of the samples were put in 5 mm diameter quartz tubes.

Static and dynamic (QELS) light scattering patterns have been measured on the same samples with a standard setup.[15] The light source was an argon ion laser ($\lambda = 488$ nm), and the procedure previously reported was followed. The angular distribution of scattered light was measured from $\theta = 10°$ to 150°; the scattering vector q was given by

$$q = (4\pi n/\lambda)\sin(\theta/2) \qquad (1)$$

with the refractive index $n = 1.33$ for water.

The scattering vector ranged from 3×10^{-3} to 3×10^{-2} nm^{-1}. The intensities, *I(q)*, were scaled by measuring the intensity scattered by benzene, *I*(benzene), under the same conditions.

Light Scattering Data Analysis. The patterns of light scattered by a solution of particles of volume *V* with refractive index *n* and volume fraction Φ is given by[32]

$$\frac{I(q)}{I(\mathrm{benzene})} = K\left[\frac{\mathrm{d}n}{\mathrm{d}\Phi}\right]^2 FVP(q)S(q) \qquad (2)$$

where the constant *K* depends on the experimental setup, *P(q)* is the form factor of the scattering objects, and *S(q)* is the structure factor. As usually, *S(q)* is assumed constant in this work over the range of wave vectors explored in the light scattering experiments.

QELS experiments give the time dependence of the polarization from which light scattering itself arises. The relaxation of the polarizability fluctuations determines therefore the spectral features. With surfactant aggregates such as vesicles, fluctuations of concentration induce polarizability fluctuations, which relax through a thermal diffusion process of the aggregates themselves. Berne and Pecora[33] and Chu[34] give the autocorrelation function of the scattered intensity as

$$C(q,t) = \langle |I(q,0)|I(q,t)| \rangle = I(q)^2(1 + b|g_1(q,t)|^2) \quad (3)$$

where the autocorrelation function of scattered electric field $g_1(t)$ is given by

$$g_1(t) = \langle |E_s(q,0)|E_s(q,t)| \rangle \quad (4)$$

In the case of diluted solutions of monodisperse, spherical vesicle, $g_1(t)$ decays exponentially, and the relaxation time in the autocorrelation function may simply be defined as

$$\tau = 1/Dq^2 \qquad D = kT/6\pi\eta r_h \quad (5)$$

with η = viscosity of the solutions, D = diffusion coefficient, and r_h = hydrodynamic radius of the scattering spherical particle.

With diluted solutions of polydisperse, noninteracting particles, a weighted sum of exponential decays can fit the experimental patterns

$$g_1(q,t) = [\sum_i K\Phi_i V_i P_i(q) \exp(t/\tau)]/\sum_i K\Phi_i V_i P_i(q) \quad (6)$$

Finally, when the size distribution is monomodal and not too large, the QELS results are interpreted with a polynomial development of $\log[g_1(q,t)]$ in order to obtain averaged values of r_h and semiquantitative indices of polydispersity.[33,34]

ESR Spectra Calculation. In microscopically ordered and macroscopically disordered (MOMD) fluid phases, such as nonoriented membranes or vesicles, the probe motion can be rapid, but the local preferential orientation of molecules prevents the modulation of the magnetic anisotropies so that ESR spectra show strongly anisotropic features.[35,36] With uniaxial order, as it happens in a smectic phase of a lipid multilayer, the anisotropies in the plane perpendicular to the preferential axis are completely averaged, so that the system may be described in terms of a single order parameter:[37]

$$S_{33} = (\langle 3\cos^2\theta \rangle - 1)/2 \quad (7)$$

where θ is the angle between the N−O bond and the axis of local director. In our calculations we chose $\theta = 0$ since in DXSA nitroxides the N−O bond, on which the director is aligned, is parallel to the alkyl chain of the nitroxide and of the surfactant molecules because of the occurring preferential ordering. An appropriate calculation procedure of the order parameter is given by Freed and co-workers[38] in terms of a reorienting potential:

$$-U(\Omega) = K_B T\lambda_0^2 P_2 \cos\beta \quad (8)$$

where $\Omega(\alpha,\beta,\gamma)$ is a Eulerian angle reference frame describing the orientation of the radical with respect to a laboratory-fixed reference system, and λ_0^2 is the largest term of the type λ_K^L in the expansion of the reorienting potential with respect to the Wigner matrix elements $D_{MK}^L(\Omega)$ as defined by Freed and coworkers.[38]

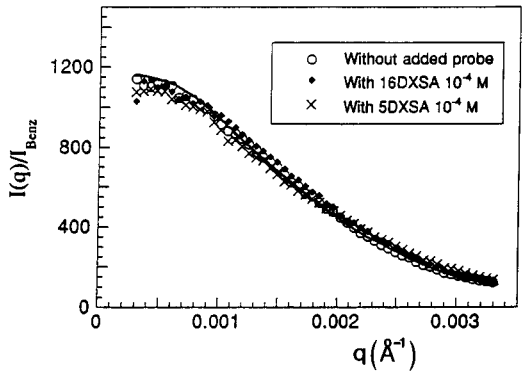

Figure 1. Static light scattering patterns of the betaine/PFPE system (total surfactant concentration 0.5%; $x_{bet} = 0.75$) in the absence of paramagnetic probes and in the presence of 5- and 16-DXSA.

On these bases, a simulation program has been written and modified in order to use a limited basis set (MOMDL, where L stands for limited). This program makes a spectral integration with respect to the tilt angle, φ, of the director against the external magnetic field. More details on the calculation procedure are found elsewhere.[39]

Results and Discussion

Light Scattering. In order to have significant ESR measurements, we had to verify that the addition of spin probes did not significantly affect the shape and size of the aggregates in the different experimental situations. It is known that the addition of foreign molecules in surfactant assemblies may introduce significant perturbations on the system under study. This is verified in particular for micelles of perfluorinated compounds.[21,27,40,41] Here we report, as an example of this approach, the static LS curves from betaine/PFPE vesicles at 0.5 w/w total concentration ($x_{bet} = 0.75$) containing 5- and 16-DXSA (Figure 1). These data are representative of a more general behavior.

The patterns were the same in the absence of probe and in the presence of 10^{-4} mol/L 5- and 16-DXSA. The simulation (full line in Figure 1) was carried out through eq 2, using the form factor of vesicles plus an isotropic contribution as $P(q)$,

$$\frac{I(q)}{I(\text{benzene})} = A\frac{\sin^2(qR)}{(qR)^2} + B \quad (9)$$

and assuming $S(q)$ in eq 2 as a constant, as reported in ref 15. In eq 9 R is the vesicle radius as determined by LS data. The values of R are not directly comparable with the above defined r_h values since the second ones are relative to the dynamic process.

From this equation a radius $R = 84$ nm was extracted ($A = 7.4 \times 10^{-4}$ and $B = 93$ were also adjustable parameters).

For more concentrated solutions (e.g. 1.27% of total surfactant) a similar behavior was observed. The simulation of the static curves of samples containing $x_{bet} = 0.79$ gave a radius of 130 ± 10 nm, in line with the data reported in ref 15, and still no significant difference in systems containing *m*-DXSA (up to 10^{-4} M) was detected. Figure 2 reports the QELS results at different angles (from 30° to 150°) for the same system in the presence and in the absence of nitroxides. Here again no difference is detected. The apparent hydrodynamic radius r_h, deduced from the mean value of $\tau^{-1}q^2$, is equal to 200 ± 20 nm. In these concentrated solutions the r_h and R values are found significantly different, contrarily to the more dilute solutions, where they are found identical within experimental errors ($r_h = 80 \pm 10$ nm and 84 ± 10 nm). The difference between R and the apparent hydrodynamic radius deduced from

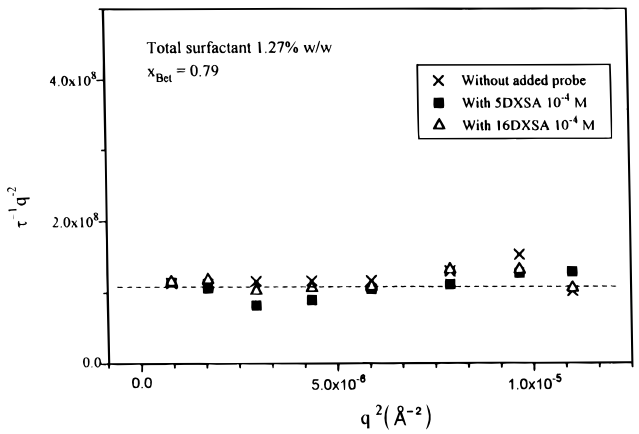

Figure 2. Quasi-elastic light scattering of the betaine/PFPE system (total surfactant concentration 1.27%; $x_{bet} = 0.79$) in the absence of paramagnetic probes and in the presence of 5- and 16-DXSA.

eq 5 may be traced back to the superposition of different mechanisms of relaxation or to a modification of D due to the interactions among vesicles. As for this latter effect, it is to be pointed out that in the system containing very large vesicles ($R > 100$ nm) a small q dependence of $S(q)$ could be reasonably expected, which would lead to the observed differences, since in the dynamic experiment the $S(q)$ influence is normally compensated by hydrodynamic interactions. However further investigations are required to ascertain the origin of the observed difference.

In summary, all of these findings proved that the insertion of nitroxide radicals did not affect the vesicles, either from a shape and size point of view (static curves) or from a dynamical point of view (QELS data).

Dynamic LS measurements were also carried out on pure betaine micellar phases containing nitroxides. Because of the presence of small and isotropic scatterers, these measurements were carried out at just one angle value (90°). The calculated values of r_h are summarized below:

nitroxide-free betaine micelle	$r_h = 2.00 \pm 0.02$ nm
5-DXSA-containing betaine micelle	$r_h = 2.00 \pm 0.02$ nm
16-DXSA-containing betaine micelle	$r_h = 2.10 \pm 0.02$ nm

ESR Spectra of *n*-DXSA in NH_4Cl Water Solution. Figure 3 shows the experimental spectra of saturated *n*-DXSA nitroxides in 0.1 M NH_4Cl water solution at $T = 295$ K. In all cases, fast motion conditions were verified, with an isotropic coupling constant of 1.58 mT, which is typical of a polar environment. No polarity profile was observed from the coupling constant values, which were the same independently on the doxyl position in the hydrocarbon chain. The same aqueous environment was therefore sensed by each nitroxide. No aggregation trend was observed at these concentrations with respect to the water environment. The dashed lines in Figure 3 show the simulated spectra, whose computational parameters are collected in Table 1. The magnetic parameters shown in Table 1 were obtained as the best-fit ones in the calculation and were in very good agreement with those extracted from ESR spectra in frozen solutions. The anisotropic magnetic parameters g and A, as well as the residual line width $T_{2,0}$, were the same, independently of the nitroxide. On the contrary, a dependence of the mobility on the position of the doxyl unit along the stearic acid chain was observed.

The calculated correlation times were somewhat anisotropic (anisotropy parameter $n = 2$), as expected for a long-axis molecule. No anisotropy was necessary to simulate the ESR

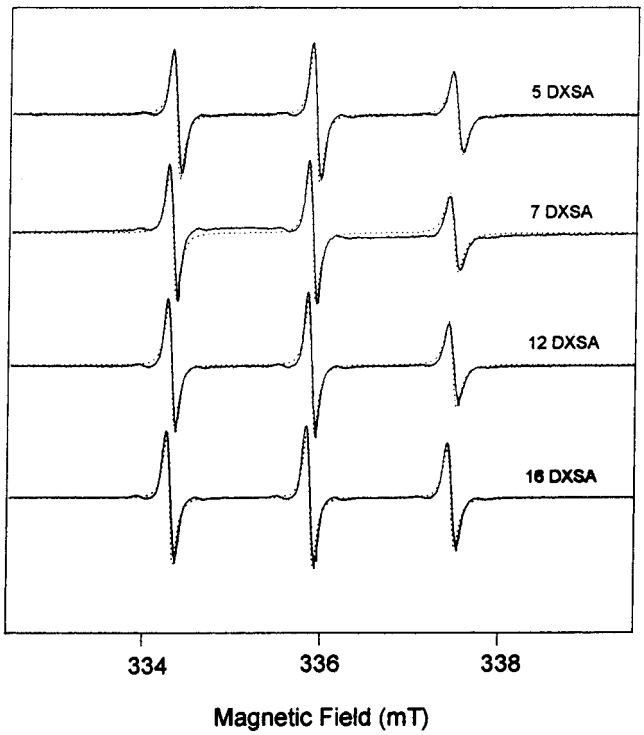

Figure 3. Experimental (full lines) and calculated (dashed lines) ESR spectra of 5-, 7-, 12-, and 16-DXSA in 0.1 mol/L NH_4Cl saturated aqueous solutions ($T = 295$ K).

spectrum of 16-DXSA; this was not surprising in light of the almost free, isotropic motion of the chain points in the terminal positions.

ESR Spectra of *n*-DXSA in the Betaine Micellar Phase. Figure 4 shows the ESR spectra of *n*-DXSA in 0.1 NH_4Cl water solution of betaine micelles (0.5% w/w corresponding to a betaine concentration of 2×10^{-2} mol/L, higher than the betaine cmc in water, 2×10^{-3} mol/L, as determined by Gauthier-Fournier[28]). From either the experimental spectra or the calculated parameters shown in Table 2, a more marked mobility profile with the doxyl position on the stearic chain resulted with respect to that observed in bulk water. As expected, the observed mean increases of τ_c from 5×10^{-10} s to 1.5×10^{-9} s on going from 16- to 5-DXSA reflected a partial immobilization of the reorientating paramagnetic unit when inserted in a surfactant aggregate, with the largest fluidity toward the center of the micelle core. Almost the same motional anisotropy as in bulk solution was necessary for a good fit of the spectra of nitroxides in betaine micelles. It is noteworthy that the coupling constant significantly changed (1.46−1.5 mT), which was well in line with a more hydrophobic environment around N−O, thus proving the insertion of the hydrophobic chain into the hydrocarbon region of the aggregate.

Figure 5 shows the temperature dependence of the ESR spectra of 5-DXSA in betaine micelles. The observed behavior of the line width was in perfect agreement with that predicted by the relaxation mechanisms governing the line shape in these nitroxides.[42,43] A similar trend was observed for the other probes. For instance, in the case of 16-DXSA a linear variation of log ΔB as a function of T was calculated in the temperature range 278−313 K (Figure 6). This indicated a monoexponential relaxation, which was interpreted as due to the rapid averaging of the magnetic anisotropies of the probe located in a single site. We were not interested in this work to determine dynamic parameters such as the activation energies, which could be calculated from the data of Figure 6. We wish only to stress here that the monoexponential behavior proved the occurrence

TABLE 1: Magnetic Parameters and Correlation Times of *n*-DXSA in NH_4Cl Water Solution at 295 K

NH_4Cl	g_{xx}[a]	g_{yy}[a]	g_{zz}[a]	A_{xx}[b] (mT)	A_{yy}[b] (mT)	A_{zz}[b] (mT)	$T_{2,0}$[b] (mT)	$<A>$[b] (mT)	τ_c[c] (s)	n
5-DXSA	2.0080	2.0062	2.0029	0.62	0.58	3.54	0.05	1.48	1.5×10^{-9}	2
7-DXSA	2.0080	2.0062	2.0029	0.62	0.58	3.54	0.05	1.50	1×10^{-9}	2
12-DXSA	2.0080	2.0062	2.0029	0.62	0.58	3.54	0.05	1.48	9×10^{-10}	2
16-DXSA	2.0080	2.0062	2.0029	0.62	0.58	3.54	0.055	1.46	4.5×10^{-10}	1.5

[a] ± 0.0003. [b] ± 0.02. [c] ± 0.2.

TABLE 2: Magnetic Parameters and Correlation Times of *n*-DXSA in Betaine Solution (2×10^{-2} M in H_2O + 0.1 M NH_4Cl) at 295 K

$x_{bet} = 1$	g_{xx}[a]	g_{yy}[a]	g_{zz}[a]	A_{xx}[b] (mT)	A_{yy}[b] (mT)	A_{zz}[b] (mT)	$T_{2,0}$[b] (mT)	$<A>$[b] (mT)	τ_c[c] (s)	n
5-DXSA	2.0083	2.007	2.0029	0.53	0.47	3.44	0.01	1.48	1.5×10^{-9}	2.55
7-DXSA	2.0083	2.007	2.0029	0.54	0.48	3.47	0.05	1.50	1×10^{-9}	1.5
12-DXSA	2.0083	2.007	2.0029	0.53	0.47	3.44	0.03	1.48	9×10^{-10}	1.5
16-DXSA	2.0083	2.007	2.0029	0.52	0.46	3.43	0.05	1.46	4.5×10^{-10}	1

[a] ± 0.0003. [b] ± 0.02. [c] ± 0.2

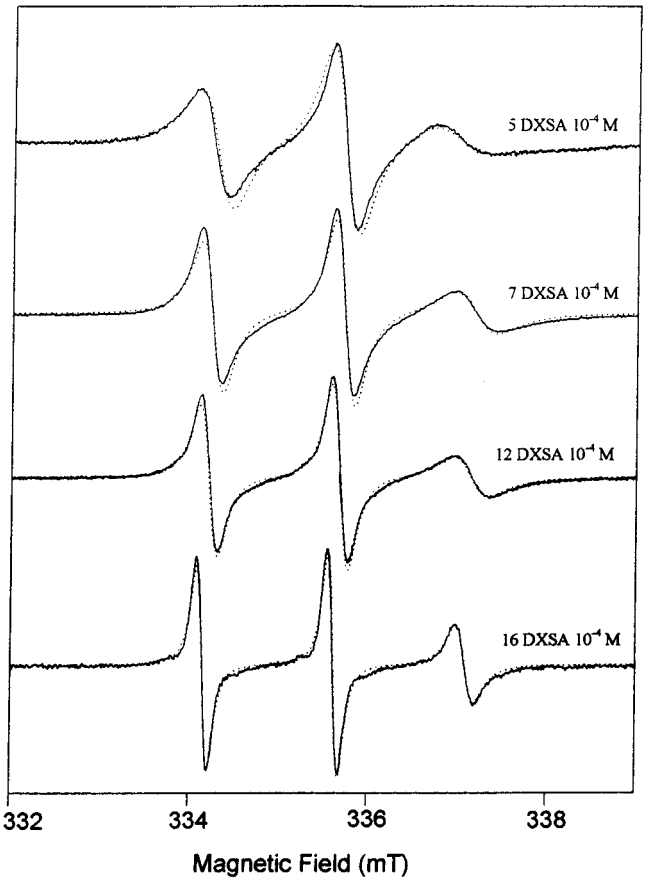

Figure 4. Experimental (full lines) and calculated (dashed lines) ESR spectra of 5-, 7-, 12-, and 16-DXSA in betaine micelle aqueous dispersions (probe concentration 10^{-4} mol/L; $T = 295$ K).

of objects of very similar sizes, containing paramagnetic probes with a "regular" dynamics which reoriented in a highly fluid environment even at relatively low temperatures. This confirmed the presence of monodisperse betaine micelles with a very fluid and substantially isotropic ($n = 1-2.5$) hydrophobic core.

The fast motion conditions were verified for 5-DXSA in betaine micelles only at temperatures higher than 290 K. Above 290 K also in this case a monoexponential behavior of the line width was observed, as expected from the dominant relaxation mechanism. Below 288 K, slow-motion spectra were observed, which corresponded to a single-valued correlation time.

ESR Spectra of *n*-DXSA in Pure PFPE Aggregates. Because of the claimed mutual phobicity between fluorinated and hydrogenated compounds,[44,45] a very slight solubility of the

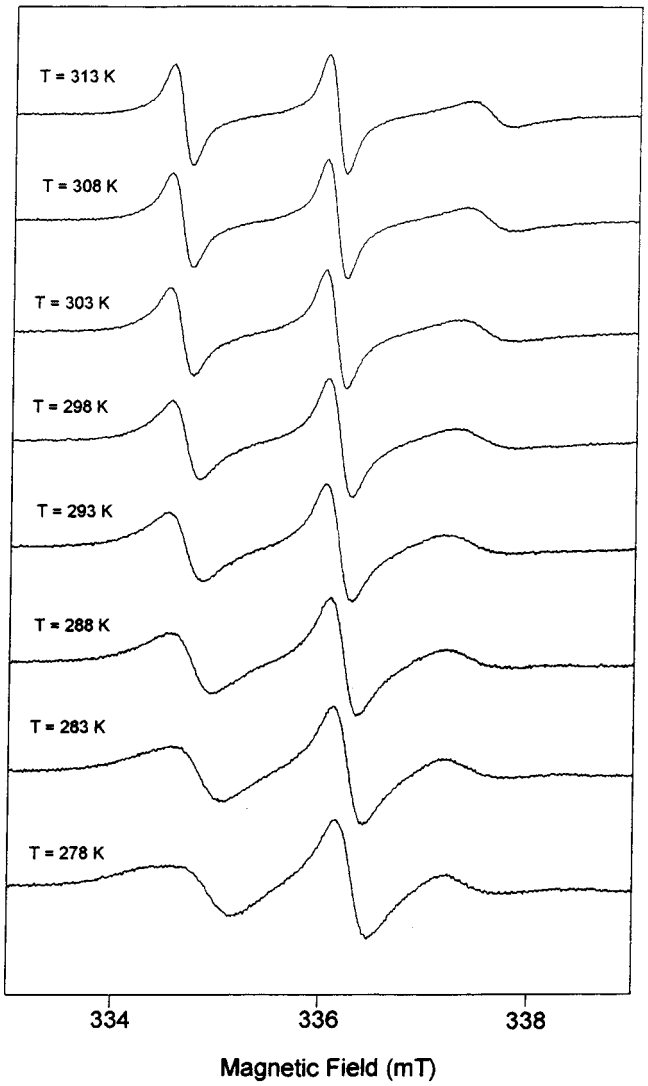

Figure 5. Experimental ESR spectra of 16-DXSA (10^{-4} mol/L) in betaine micelle aqueous dispersions ($NH_4Cl = 0.1$ mol/L) at different temperatures.

nitroxide probes was expected in PFPE aggregates. This is verified in particular with 5- and 7-DXSA as it results from Figure 7, which shows the experimental ESR spectra of the different nitroxides introduced in aqueous dispersions of PFPE (total concentration 0.5% w/w). In the cases of 5- and 7-DXSA the experimental spectra were clearly due to a superposition of at least two different absorptions arising from radicals located in hydrophobic and hydrophilic environments. The second one

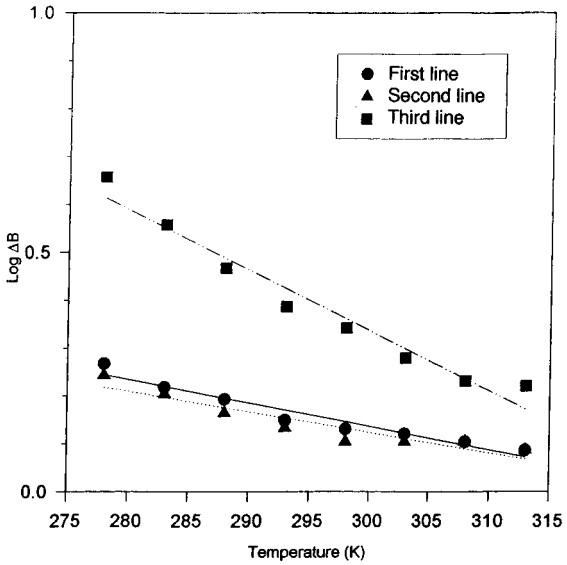

Figure 6. Variation with temperature of the line width of the three components of the 16-DXSA spectrum in aqueous (0.1 mol/L NH_4Cl) dispersions of betaine micelle.

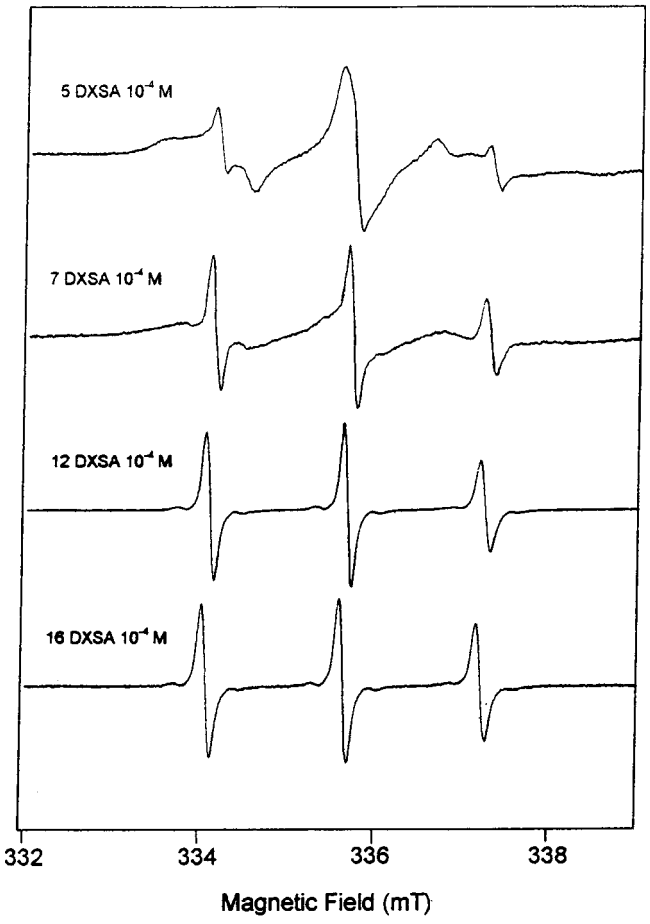

Figure 7. ESR spectra of 5-, 7-, 12-, and 16-DXSA inserted in PFPE aggregates (surfactant concentration 0.5% w/w) in aqueous (0.1 mol/L NH_4Cl) dispersions.

could be the bulk water component, although the complexity of the spectra did not allow us to separate the components in a simple manner. Structural data, mainly from small-angle scattering (namely, SAXS and SANS) and light scattering techniques, indicate the existence of polidisperse aggregates, probably including multilamellar vesicles.[15−17,41] The 12- and 16-DXSA spectra were simulated with the same parameters as

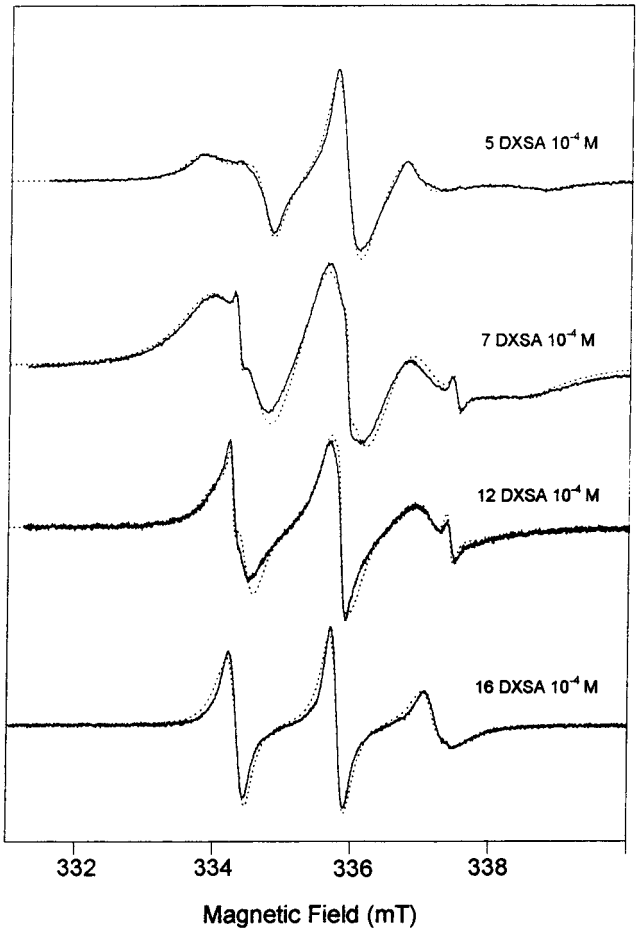

Figure 8. Experimental (full lines) and calculated (dashed lines) ESR spectra of 5-, 7-, 12-, and 16-DXSA inserted in aqueous dispersions of mixed betaine/PFPE vesicles (total surfactant concentration 0.5% w/w; $x_{bet} = 0.79$; $NH_4Cl = 0.1$ mol/L; $T = 295$ K).

in bulk water, thus suggesting that very weak interactions arose from these species and PFPE aggregates.

ESR Spectra of *n*-DXSA in Mixed Betaine/PFPE Vesicles. Figure 8 collects the experimental and simulated spectra of *n*-DXSA in mixed betaine/PFPE vesicles. Table 3 reports the best-fit values obtained for the simulations. The magnetic parameters were in good agreement with those obtained from 100 K frozen spectra. The betaine/PFPE molar fraction used for these spectra was 0.75, and the total surfactant concentration 0.5% w/w. Light scattering measurements indicated that at this molar ratio and at this total surfactant concentration, monodisperse, unilamellar vesicles of radii of 84 nm prevailed.[15] The modulation of the magnetic anisotropies in the signal from the 5-DXSA nitroxide in a position that was located near the water/bilayer interface was clearly incomplete. The partial resolution of the $A_{||}$ hyperfine component suggested a location of the probe in an environment with a preferential ordering. This absorption was simulated with $\langle \tau_c \rangle = 2 \times 10^{-9}$ s, with an appreciable anisotropy parameter ($n = 10$), with $\tau_{c\perp} > \tau_{c||}$, and by introducing a reorienting potential, according to eq 8, with $\lambda = 1.8$. This resulted in an order parameter along the local director axis, as defined in eq 7, $S_{33} = 0.4$. This meant that an appreciable order degree was sensed by the radical in a position in proximity of the bilayer surface. The order parameter, as expected, decreased with the sinking of the N−O group into the hydrophobic part of the bilayer.

The $\langle A_N \rangle$ value of 1.47 mT is almost the same as that observed in betaine micelles. This was true for all the nitroxides used.

TABLE 3: Magnetic Parameters, Correlation Times, and Order Parameters of *n*-DXSA in Mixed Betaine/PFPE Vesicles at 295 K

$x_{bet} = 0.75$	g_{xx}[a]	g_{yy}[a]	g_{zz}[a]	A_{xx}[b]	A_{yy}[b]	A_{zz}[b]	$T_{2.0}$[b]	$<A>$[b]	τ_c (s)[c]	λ	S_{33}	n
5-DXSA	2.0083	2.007	2.0029	0.52	0.46	3.43	0.12	1.47	2×10^{-9}	1.8	0.4	10
7-DXSA	2.0083	2.007	2.0029	0.52	0.46	3.43	0.12	1.47	1.5×10^{-9}	1.4	0.31	16
12-DXSA	2.0083	2.007	2.0029	0.52	0.46	3.43	0.15	1.47	1.5×10^{-9}	0.8	0.17	20
16-DXSA	2.0083	2.007	2.0029	0.52	0.46	3.43	0.12	1.47	8×10^{-10}	0.5	0.10	20

[a] ±0.0003. [b] ±0.02. [c] ±0.2.

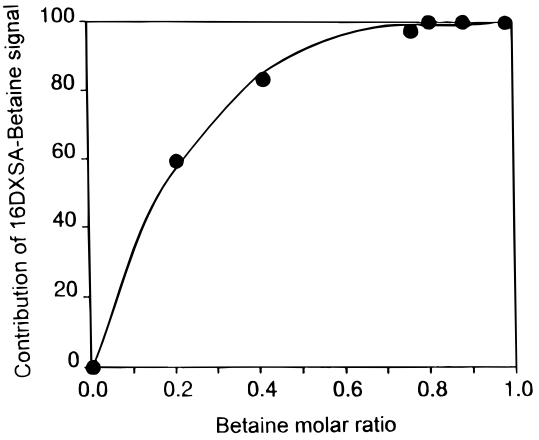

Figure 9. Variation of the contribution of the intensity from 16-DXSA absorption in betaine environment as a function of the betaine molar fraction ($T = 295$ K).

The 7-DXSA spectrum was certainly more complex than that of 5-DXSA. Two components at least were identified in this spectrum as due to radicals moving in different motional domains. The broad absorption with incomplete modulation of the anisotropies showed strong analogies with that of 5-DXSA. It was therefore to be attributed to radicals buried in regions of very restricted motion and was simulated with the same magnetic parameters as in water. These components, which were also present in 12- and 16-DXSA spectra, were summed up with partition coefficients dependent on the nature of the nitroxide and on the betaine content of the system.

We could say at this point that the signal behavior of the four probes, once inserted into the closed bilayer characterized by microscopic order, sensed conditions of motion not sufficiently fast to completely average the anisotropies, and the simulation allowed us to separate the absorptions arising from nitroxides inserted into a betaine-rich fraction bilayer (betaine signal) from that localized in an almost pure water environment (water signal).

Figure 9 shows the variation of the relative intensity of the betaine/16-DXSA signal against the betaine molar fraction. This variation was described by third rank polynomial behavior, thus indicating the marked tendency of the radical to localize in a hydrogenated phase with the increase of the betaine content in the system; for example, at $x_{bet} = 0.4$, the betaine signal fraction is >80% and the trend toward unity was very rapid. The data reported in Figure 9 clearly suggested that by passing from PFPE aggregates to betaine micelles through vesicle formation, the probe progressively changed its environment from a pure water environment to a betaine environment, which therefore occurred as an almost separate domain in the mixed PFPE/betaine vesicles. The spectra at betaine/PFPE ratios 0.7−0.8, typical of the vesicles, were simulated with contributions of betaine spectra higher than 96−97%. This was therefore a very clear proof of the occurrence of separate surfactant domains in the mixed vesicles.

The above behavior was also shown by the other nitroxides.

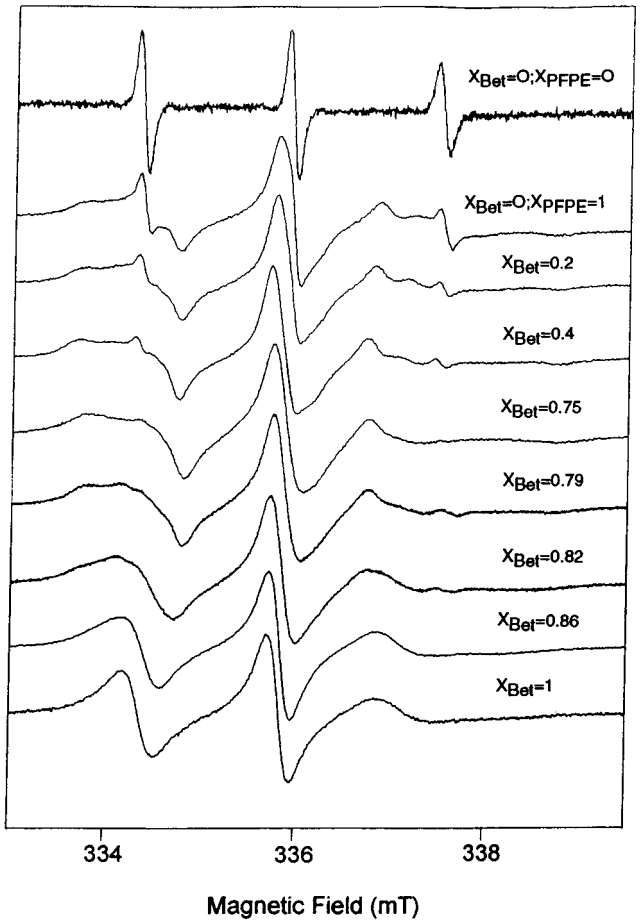

Figure 10. ESR spectra of 5-DXSA (10^{-4} mol/L) as a function of the betaine/PFPE ratio (from pure aqueous phase to $x_{bet} = 1$; $T = 295$ K).

Figure 10 shows the 5-DXSA line shape change going from pure PFPE aggregates to pure betaine micelles in a total surfactant concentration 0.5% w/w. The ESR spectrum of 5-DXSA in 0.1 M NH_4Cl water solutions is also shown as a comparison. The increase of the betaine fraction led to a decrease of the contribution of absorptions other than that in a betaine environment. In addition, the occurrence of structurally different aggregates was indicated by the line shapes. A partial resolution of the parallel hyperfine components was observed in the presence of mono- and polydisperse vesicles ($x_{bet} = 0.2-0.8$), whereas a progressive increase of the mobility was observed when betaine micelles were predominant ($x_{bet} > 0.82$). In this case too the spectral trend was indicative of the different order degree that characterized the vesicle and micelle aggregates. From a more careful inspection of the ESR spectra at $x_{bet} = 0.79$, the signal from micelles began to gain intensity with respect to the slow motion spectrum which was attributed to vesicles. This was most probably due to the presence of micelles that escaped from a direct scattering revelation and only appeared as an isotropic background in the static LS.[15]

Analysis of the ESR Spectra from PFPE−Tempamide. The 298 K ESR spectrum of PFPE−Tempamide in 0.1 M NH_4

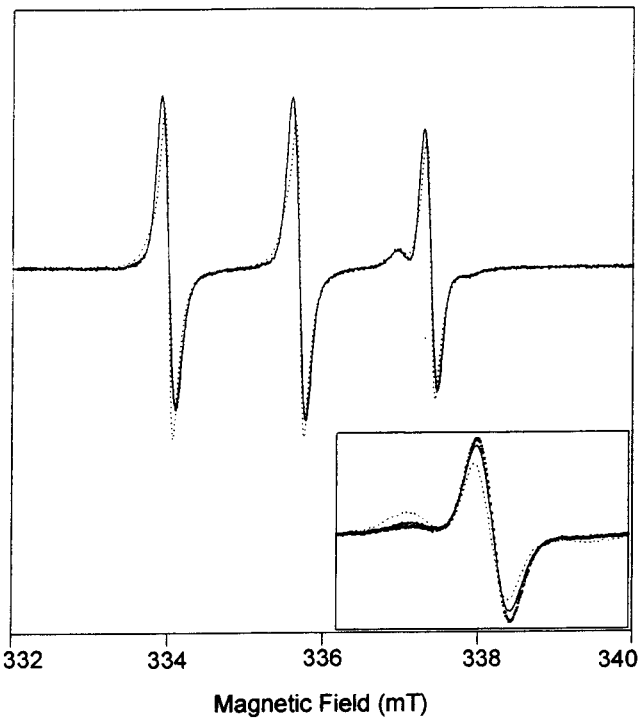

Figure 11. Experimental (full line) and calculated (dashed line) ESR spectrum at 295 K of the PFPE−Tempamide radical inserted in a 0.5% w/w dispersion of PFPE in 0.1 mol/L NH_4Cl aqueous solution. Inset: Changes of the third line of the above spectrum as a function of the total PFPE concentration.

Cl water solution was the classical well-resolved three-line pattern under the condition of very rapid motion. This spectrum was reproduced with $\tau_c = 2 \times 10^{-11}$ s, which is a very high mobility of the paramagnetic unit with respect to the molecular size. This was not unexpected since it is known that the correlation time reflects the motion of the paramagnetic unit instead of that of the molecule as a whole. The high coupling constant value (1.69 mT) reflected an almost pure aqueous environment around the −N−O unit. Figure 11 shows the experimental (full line) and computed (dashed line) spectra of PFPE−Tempamide inserted in PFPE aggregates (total surfactant concentration = 0.5% w/w). The overall spectrum was due to the superposition of two spectra with different mobility and different magnetic parameters, particularly the hyperfine coupling constant A_N. This fact was clearly observed from the high-field absorption, whose feature at different PFPE concentration is shown in the inset of Figure 11. The probe was therefore localized in two different regions with different motional properties, the slower one whose intensity increased with the increase of PFPE content. For a deeper investigation of this aspect, pure lamellar dispersions of PFPE were investigated with this probe. Figure 12 shows both experimental and simulated spectra of PFPE−Tempamide in water dispersions of PFPE at a concentration (10% w/w in water) where practically only lamellae are know to exist.[16,17] The magnetic parameters that fitted the experimental pattern were as follows:

$$g_{xx} = 2.0095 \qquad A_{xx} = 1.05 \text{ mT}$$

$$g_{yy} = 2.0068 \qquad A_{yy} = 1.05 \text{ mT}$$

$$g_{zz} = 2.0029 \qquad A_{zz} = 2.91 \text{ mT}$$

$$T_{2,0} = 0.12 \text{ mT} \qquad \langle\tau_c\rangle = 5 \times 10^{-11} \text{ s} \qquad \lambda = 1.5 \qquad n = 50$$

to be compared with the following fitting parameters used for the spectrum in aqueous solution:

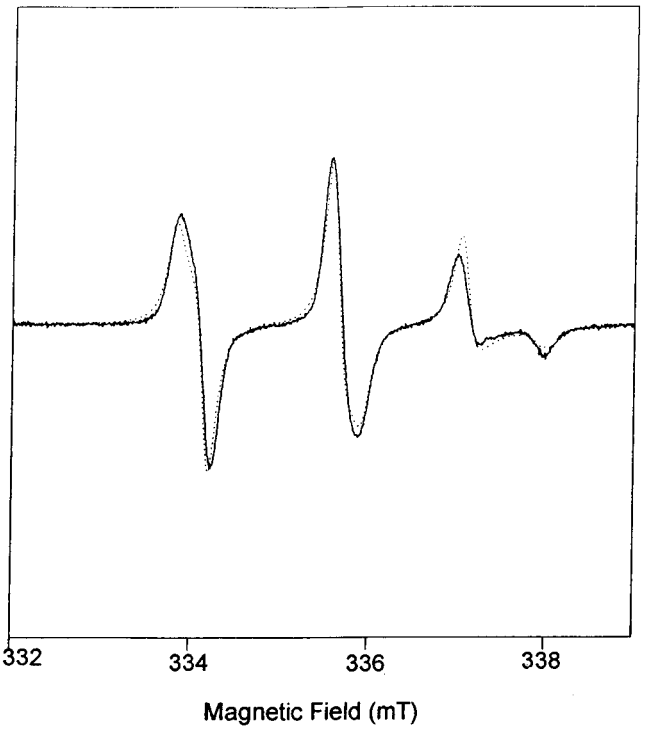

Figure 12. Experimental (full line) and calculated (dashed line) ESR spectra of the PFPE−Tempamide radical (10^{-4} mol/L) imbedded into lamellar phases of PFPE in water (PFPE concentration 10% w/w; T = 295 K).

$$g_{xx} = 2.0095 \qquad A_{xx} = 0.69 \text{ mT}$$

$$g_{yy} = 2.0068 \qquad A_{yy} = 0.62 \text{ mT}$$

$$g_{zz} = 2.0029 \qquad A_{zz} = 3.76 \text{ mT}$$

$$T_{2,0} = 0.1 \text{ mT} \qquad \tau_c = 2 \times 10^{-11} \text{ s} \qquad \lambda = 0 \qquad n = 0$$

The values $\lambda = 1.5$ and $n = 50$ used for the simulation of the PFPE−Tempamide spectrum in lamellar PFPE phases ensured a strong anisotropy; that is, the probe was well matched with its fluorinated tail within the PFPE surfactant molecules forming the bilayer, whereas the polar nitroxyl head sensed a pure aqueous environment outside the multilayer itself, with a motion frequency and coupling constant value not far from those in pure water.

The experimental spectra have therefore been simulated as the sum of the signal from the probe in 0.1 mol/L NH_4Cl pure water solution and the signal from the probe in lamellar multilayers. The simulation of the signals shown in the inset of Figure 12 was carried out as the sum of the above spectra with the following contributions depending on the PFPE concentrations:

% w/w	lamellar phase (%)	aqueous phase (%)
1.27	95	5
0.50	87	13
0.25	78	22

When this probe was inserted into mixed betaine/PFPE vesicles, the overall line shape was very similar to that observed in a 0.1 mol/L NH_4Cl solution. A small difference, due to the superposition of different spectra as described above, was only observed in the samples with a total concentration of surfactants $\geq$0.5% w/w. As for the cases in PFPE aggregate solutions, these spectra were therefore interpreted as due to the sum of

Figure 13. (*a*, top) Proton NMR spectrum at 200 MHz of a 9.84×10^{-4} (below cmc) mol/L dodecylbetaine solution in D_2O (NH_4Cl = 0.1 mol/L). (*b*, bottom) Proton NMR spectrum at 200 MHz of a 1.8×10^{-2} mol/L (above cmc) dispersion of dodecylbetaine in D_2O (NH_4Cl = 0.1 mol/L).

the paramagnetic amide inserted in the fluorinated domain of the vesicle in almost fast, isotropic motion because of the fast rotation around the amide bond. The computation of a such situation was not accomplished because of the very small spectral changes arising from relatively small contributions of the slow-moving species.

NMR Spectra. Lyotropic liquid crystal phases have been widely investigated through NMR, because of the ability of this spectroscopic method to give details on the molecular organization of surfactant aggregates, since in these systems the tensor interactions (dipolar, quadrupolar, chemical shift, etc.) are not completely averaged, thus contributing to the static spin Hamiltonian and affecting the energy levels of the spin state.[46] With ^1H as the NMR active nucleus, no quadrupolar effects and very small chemical shift anisotropy are expected. The major source of relaxation of ^1H in surfactant liquid crystal phases is thus determined by inter- and intramolecule dipolar interactions which are averaged out by the molecular motion. The intramolecular dipolar couplings of static nature result in a super-Lorentzian absorption shape,[47] whereas the intermolecular effects are averaged out by the rapid translational and rotational motions of the surfactant molecules. The size increase leads to faster transverse relaxation rate.[48] The size increase of micelles, for instance, shows broadening of the bands.

Figure 13a shows the 295 K ^1H-NMR spectrum obtained at 200 MHz from a betaine solution in D_2O at concentration of 9.84×10^{-4} mol/L (lower than cmc) and containing 0.1 mol/L

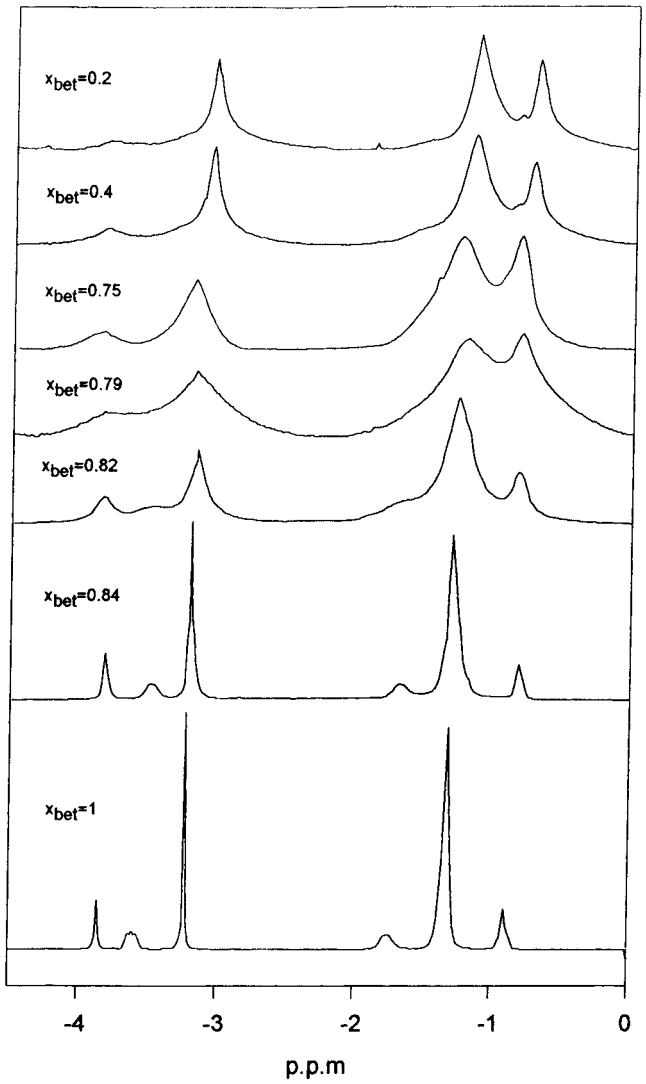

Figure 14. NMR spectra of the betaine/PFPE system as a function of the betaine content ranging from pure betaine to $x_{bet} = 0.2$.

NH_4Cl. The peak assignment was based on the assignment reported by König[49] at 60 MHz for the same compound in brine-free water:

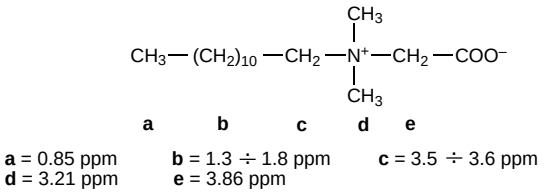

Figure 13b shows the 200-MHz spectrum of betaine micelles ($c = 1.8 \times 10^{-2}$ mol/L). The most appreciable difference in the spectra reported in Figure 13 resided in a larger width of some of the lines obtained in the micellar phase, namely, the peaks around 3.5 and 1.3 ppm. This agreed perfectly with the monomer−micelle transition, that is, with the betaine molecules passing from a totally disordered environment where the motion is free (monomer state) to a less disordered environment (the micellar aggregate) where the motion is hindered to a certain extent.

Figure 14 shows the NMR spectra of the betaine/PFPE system as a function of the betaine content ranging from pure betaine to $x_{bet} = 0.2$, that is, in the range where betaine micelles, monolamellar betaine/PFPE vesicles, and other ill-defined mixed

aggregates existed. A further weak line broadening with respect to pure betaine micelles was observed at $x_{bet} = 0.84$, where LS data indicate the occurrence of larger mixed micelles.[15] The spin relaxation became more efficient, with a marked line broadening, in the samples containing betaine with $x_{bet} = 0.82-0.75$, where, as shown by scattering data, a transition occurred with the appearance of large vesicles, whose wide absorption was superimposed to the narrow signals from micellar and premicellar aggregates. At $x_{bet} = 0.79-0.75$ vesicles of $r_h = 80-90$ nm were practically the only supramolecular structure present in the systems and the observed spectra were the widest spectra.

Betaine molecules in the vesicle bilayers behaved as in liquid crystals, namely, in a lamellar phase. However it has been argued[50] that in vesicles the line width is narrower than in the corresponding smectics because the faster Brownian reorientational motion in vesicles is able to better average the magnetic anisotropies. The uniassic-type order was however higher than in the hydrophobic core of the micelles, where the hydrocarbon chains behaved as liquid-like chains.[51]

No large chemical shift was apparent in these spectra, which meant that the environment around betaine molecules in the vesicles was not very different from the environment sensed in pure betaine micelles. The small increase of PFPE content from $x_{bet} = 0.79$ to 0.75 had the only effect of increasing the hydrodynamic radius of the rotating object without changes in its domain composition and separation.

Below $x_{bet} = 0.5$, the NMR line width showed again an overall decrease, with possible superposition of different signals. This was in line with the scattering data that suggested the existence of polydisperse vesicles (with large spreading of size) and other PFPE aggregates.

The same overall considerations might be made in the interpretation of the NMR results from samples with total surfactant concentrations 0.25% and 1.27% (w/w).

Conclusion

Pure betaine micelles and mixed vesicles of betaine with a perfluorinated surfactant, whose behavior in solution is known, have been studied by LS, ESR, and NMR. All of these techniques converged in defining the narrow concentration range, in which mixed, unilamellar, monodisperse vesicles occurred. These systems are stable and may be the basis for the preparation of suitable carriers of drug and biological molecules. In particular, mixed vesicles with a hydrodynamic radius in the range 80−100 nm occurred at $x_{bet} = 0.75-0.79$, when the total surfactant concentration was 0.25−0.5% w/w. The results presented here allowed us to suggest an explanation of the problem how aggregates as those described could have positive (external) and negative (internal) curvatures that led to the spontaneous formation of vesicles. The ESR line shapes of hydrogenated spin probes (*n*-DXSA, with the doxyl unit in different positions along the stearic acid chain) clearly suggested the occurrence of an ordered betaine domain separated from the PFPE domain. Indeed, the following considerations were derived from the ESR data.

(a) The hydrogenated probes were soluble in the betaine micelles, and the mobility of the doxyl unity depended on the location along the stearic acid chain; that is, the mobility increased from the region near the surface toward the center of the micelle. A substantially disordered environment was evidenced by all the probes in the micelles.

(b) An appositely tailored perfluorinated spin probe gave information on the occurrence of lamellar aggregates in pure PFPE systems. From the spectral shape analysis it was possible to separate contributions from lamellar and aqueous phases.

(c) The hydrogenated probes in mixed vesicles proved the occurrence of betaine-rich regions, where they localized. These domains showed a dynamics typical of macro-disordered and micro-ordered systems, as it is usually observed in double layers. This finding was, at least qualitatively, confirmed by the perfluorinated probe.

(d) Signals arising from micelles that coexisted with vesicles were detected (see Figure 10) at PFPE/betaine composition near the transition from vesicles to mixed micelles, as indicated by LS data.[15]

Other cases have been reported where the use of ESR of spin probes distinguished different domains of surfactants in self-organized systems. Kamogawa and Tajima[52] have studied mixed micelles of either sodium perfluorooctanoate or ammonium perfluorononanoate with sodium dodecylsulfate. From the variation of the correlation time for the motion as a function of surfactant concentration, these authors suggest the presence of two kinds of micelles, which are consistent with the freely miscible and partially immiscible micelles in the Shinoda theory.[53] The regions of existence of two micellar phases are separated by an invariant region so that two phases can also arise from the single micelles having two specific sites. In the authors' model a single kind of micelle exists at the invariant region, consisting of two micellar sites.

Additional proof of the simultaneous presence of different types of aggregates in these systems (vesicles and large micelles) was given by 200-MHz ^{1}H-NMR spectroscopy of betaine. In the composition range where vesicles prevail, the marked line broadening with loss of hyperfine resolution in the betaine spectrum was due to strong dipole−dipole interactions.

On the basis of the above considerations, the mixed betaine/PFPE vesicles might be sketched as a curved bilayer supramolecular structure, where the opposite layers are mainly fabricated by betaine and PFPE molecules, respectively. Because of packing parameters of the betaine molecule, a betaine-rich layer in the presence of a small fraction of PFPE molecules may assume a positive small curvature. The opposite happens to the PFPE-rich layer, which therefore assumes a negative curvature. This eventually allows the plane bilayer to be closed.

Acknowledgment. The authors are particularly grateful to Prof. I. Bertini for the use of European NMR Large Scale Facility. Financial supports from Italian Ministero della Universitá e della Ricerca Scientifica e Tecnologica (MURST), from Consiglio Nazionale delle Ricerche (CNR), and from Ausimont SpA allowed this work to be carried out, and these institutions are acknowledged.

References and Notes

(1) Cantú, L.; Corti, M.; Musolino, M.; Salina, P. *Europhys. Lett.* **1990**, *13*, 551.

(2) Cantú, L.; Corti, M.; Del Favero, E.; Raudino, A. *J. Phys. I* **1994**, *4*, 1587.

(3) Kaler E. W.; Herrington, K. L.; Murthy, A. K.; Zasadzinski, J. A. *J. Phys. Chem.* **1992**, *96*, 6698.

(4) Hoffmann H.; Thunig, C.; Munkert, U.; Meyer, H. W.; Richter, W. *Langmuir* **1992**, *8*, 2629.

(5) Thunig, C.; Platz, G.; Hoffmann, H. *Springer Proc. Phys.* **1992**, *66*, (Struct. Conform. Amphiphilic Membr.) 266−274.

(6) Oberdisse, J.; Couve, C.; Appell, J.; Berret, J. F.; Ligoure, C.; Porte, G. *Langmuir* **1996**, *12*, 1212.

(7) Ambuhl, M.; Bangerter, F.; Luisi, P. L.; Skrabal, P.; Watake, K. *Langmuir* **1993**, *9*, 36.

(8) Hervé, J.; Roux, A. M.; Nallet, F. and Gulik-Krywcki, T. *J. Phys.* **1993**, *3*, 1255.

(9) Riess, J. G.; Frezard, F.; Greiner, J.; Krafft, M. P.; Santaella, C.; Vierling, P.; Zarif, L. *Handbook Non-Med. Appl. Liposomes* **1996**, *3*, 97.

(10) Riess, J. G.; Krafft, M. P. *Chem. Phys. Lipids* **1995**, *75*, 1.
(11) Riess, J. G. *New J. Chem.* **1995**, *19*, 891.
(12) Kunitake, T.; Okahata, Y.; Yusunami, S. *J. Am. Chem. Soc*. **1982**, *104*, 5547.
(13) Gross, U.; Kolditz, L.; Papke, G.; Rudiger, S. *J. Fluor. Chem*. **1991**, *53*, 163.
(14) Trabelsi, H.; Szonyi, S.; Gaysinski, M.; Cambon, A.; Watske, H. J.; *Langmuir* **1993**, *9*, 1201.
(15) Ristori, S.; Appell, J.; Porte, G. *Langmuir* **1996**, *12*, 686.
(16) Gebel, G.; Ristori, S.; Loppinet, B.; Martini, G. *J. Phys. Chem.* **1993**, *97*, 8664.
(17) Ristori, S.; Gebel, G.; Visca, M.; Martini, G. *Proc. Colloid Polym. Sci.* **1993**, *93*, 337.
(18) Ristori, S. Ottomani, E.; Martini, G. *J. Phys. Chem.* **1995**, *99*, 9876.
(19) Ristori, S.; Ottomani, E.; Romanelli, G.; Martini, G. *J. Phys. Chem.*, **1995**, *99*, 17886.
(20) Martini, G.; Ristori, S.; Visca, M. In *Physical Chemistry of Ionomers*; Schlick, S., Ed.; CRC Press: Boca Raton, 1996, pp 219−250.
(21) Ristori, S.; Martini, G.; Schlick, S. *Adv. Colloid Interface Sci.* **1995**, *57*, 65.
(22) Marignan, J.; Gauthier-Fournier, F.; Appell, J.; Akoum, Y.; Lang, J. *J. Phys. Chem*. **1988**, *92*, 440.
(23) Fattal, D. R.; Andelman, D.; Ben-Shaul, A. *Langmuir* **1995**, *11*, 1154.
(24) Safran, S. A.; Pincus, P. A.; Andelman, D.; MacKintosh, F. C. *Phys. Rev.* **1991**, *43*, 1071.
(25) Koslow, M. M.; Helfrich, W. *Langmuir* **1992**, *8*, 2792.
(26) Porte, G.; Ligoure, C. *J. Chem. Phys*. **1995**, *102*, 4290.
(27) Ristori, S.; Ottaviani, M. F.; Lenti, D.; Martini, G. *Langmuir* **1991**, *7*, 1958.
(28) Gauthier-Fournier, F. Thesis, University Montpellier II, France, 1986.
(29) Ristori, S. Unpublished results.
(30) Piacenti, F.; Camaiti, M. *J. Fluorine Chem*. **1994**, *68*, 227.
(31) Ristori, S.; Rossi, S.; Ricciardi, G.; Martini, G. *J. Phys. Chem.*, submitted for publication.
(32) Candau, S. J. *Surfactant Solutions. New Methods of Investigation*. In *Surfactant Science Series*; Zana R., Ed.; M. Dekker: New York, 1989; Vol. 22, p 147.
(33) Berne, B. J.; Pecora, R. *Dynamic Light Scattering*; Wiley: New York, 1976.
(34) Chu, B. *Laser Light Scattering*, Academic Press: New York, 1991.
(35) Hemminga, M. *Chem. Phys. Lipids* **1983**, *32*, 323.
(36) Meirovitch, E.; Freed, J. H. *J. Phys. Chem.* **1980**, *84*, 3281.
(37) Seelig, J. *J. Am. Chem. Soc.* **1970**, *92*, 3881.
(38) Schneider, D. J.; Freed, J. H. In *Biological Magnetic Resonance. Spin Labeling: Theory and Applications*; Berliner, L. J., Reuben, J., Eds.; Plenum Press: New York, 1969; Vol. 8, p 1, and references therein.
(39) Meirovitch, E.; Nayeem, A.; Freed, J. *J. Phys. Chem.* **1984**, *88*, 4995.
(40) Ristori, S.; Martini, G. *Langmuir* **1992**, *8*, 1937.
(41) Martini, G.; Ristori, S.; Gebel, A.; Chittofrati, A. *Appl. Magn. Reson.* **1994**, *6*, 29.
(42) Kivelson, D. J. *J. Chem. Phys.* **1960**, *33*, 1094.
(43) Bertini, I.; Luchinat, C.; Martini, G. In *Handbook of Electron Spin Resonance*; Poole, C. P., Jr., Farach, H. A., Eds.; American Institute of Physics: Cochester, VT, 1994; Chapters III and IV, and references therein.
(44) Mukerjee, P.; Mysels, K. *ACS Symp. Ser.* **1975**, *9*, 239.
(45) Mukerjee, P. *Colloids Surf. A* **1994**, *84*, 1.
(46) Lindblom G. *Curr. Opin. Colloid Interface Sci.* **1996**, *1*, 287 and references therein.
(47) Wennerström, H. *Chem. Phys. Lett.* **1973**, *18*, 41.
(48) Wennerström, H.; Lindblom, G. *Q. Rev. Biophys.* **1977**, *10*, 67.
(49) König, H. *Z. Anal. Chem.* **1979**, 359.
(50) Finer, E. G. *J. Magn. Reson*. **1974**, *13*, 75.
(51) Bloom, M.; Burnell, E. E.; MacKay, L. A.; Nichol, C. P.; Valic, M. I.; Weeks, G. *Biochemistry* **1978**, *17*, 5750.
(52) Kamogawa, K; Tajima, K. *J. Phys. Chem.* **1993**, *97*, 9506.
(53) Shinoda, K.; Namura, T. *J. Phys. Chem.* **1980**, *84*, 365.